

Antonio Fernández, Guillermo H. Kaufmann, Ángel F. Doval, Jesús Blanco-García and José L. Fernández, "Comparison of carrier removal methods in the analysis on TV holography fringes by the Fourier transform method," *Opt. Eng.* 37(11) 2899–2905 (November 1998)

Copyright 1998 Society of Photo-Optical Instrumentation Engineers.

This paper was published in "Optical Engineering" and is made available as an electronic reprint with permission of SPIE. One print or electronic copy may be made for personal use only. Systematic or multiple reproduction, distribution to multiple locations via electronic or other means, duplication of any material in this paper for a fee or for commercial purposes, or modification of the content of the paper are prohibited.

<http://dx.doi.org/10.1117/1.601980>

Comparison of carrier removal methods in the analysis of TV holography fringes by the Fourier transform method

Antonio Fernández, MEMBER SPIE
Universidade de Vigo
Departamento de Física Aplicada
ETSEIM Lagoas-Marcosende 9
E-36200 Vigo
Spain
E-mail: antfdez@uvigo.es

Guillermo H. Kaufmann, MEMBER SPIE
Consejo Nacional de Investigaciones
Científicas y Técnicas y Universidad
Nacional de Rosario
Instituto de Física de Rosario
Bv. 27 de Febrero 210 Bis
2000 Rosario
Argentina

Ángel F. Doval
Universidade de Vigo
Departamento de Física Aplicada
ETSEIM Lagoas-Marcosende 9
E-36200 Vigo
Spain

Jesús Blanco-García
Universidade de Vigo
Departamento de Física Aplicada
ETSEIM Lagoas-Marcosende 9
E-36200 Vigo
Spain

José L. Fernández
Universidade de Vigo
Departamento de Física Aplicada
ETSEIM Lagoas-Marcosende 9
E-36200 Vigo
Spain

1 Introduction

The Fourier transform method (FTM) of fringe pattern analysis was first demonstrated by Takeda et al.¹ in 1982, and it has become one of the most popular phase evaluation methods used in high accuracy measurement systems. The FTM outstrips temporal phase measurement methods mainly in that all the information required to reduce an interferogram to a phase map is recorded simultaneously.² This means that rapid temporal phase variations can be measured. The influence of several error sources in the FTM has been extensively studied and different solutions for each particular error source have been proposed.²⁻⁹ Removal of the phase due to the spatial carrier is a key step in fringe analysis by the FTM because it can give rise to significant errors in the retrieved phase. However, phase errors associated with the existing methods of carrier removal

Abstract. Carrier removal is a key step in the Fourier transform method (FTM) of fringe pattern analysis because it can give rise to significant errors in the recovered phase. The existing methods of fringe carrier removal in the FTM are reviewed and a comparison of three different methods, translation of the sidelobe to the frequency origin, least-squares fit and subtraction of the phase of the undeformed carrier fringes, are presented. Computer-generated fringe patterns are used to determine the differences between the original and the retrieved phase distributions. Several figures of merit are proposed to assess the performance of the mentioned methods. Experimental fringe patterns, obtained by double-pulsed-subtraction TV holography, are analyzed by the methods considered here, and the retrieved phase distributions are also compared. © 1998 Society of Photo-Optical Instrumentation Engineers. [S0091-3286(98)00211-6]

Subject terms: Fourier transform method; fringe analysis; TV holography; electronic speckle pattern interferometry; speckle metrology.

Paper 980009 received Jan. 12, 1998; revised manuscript received June 17, 1998; accepted for publication June 23, 1998.

have not been quantified. In this paper, three different methods of fringe carrier removal in the FTM are compared. Computer-generated fringe patterns are analyzed by these three methods to accurately determine the differences between the original and the retrieved phase distributions. Several parameters are used to quantitatively assess the performance of each method. In addition, experimental fringe patterns obtained by double-pulsed-subtraction TV holography are also analyzed by these three methods, and the retrieved phase distributions are compared.

2 Carrier Removal in Fourier Transform Fringe Analysis

In this section, a brief review of the fringe carrier removal methods that have appeared in the literature is presented.

These methods can be classified according to the domain in which the carrier is removed,¹⁰ either the Fourier or the spatial domains.

Takeda et al.¹ removed the carrier phase in the Fourier plane by translating the sidelobe to the frequency origin (TSFO), and then computing the inverse Fourier transform. A major drawback due to the digitization of the data arises in applying this method, because the translation is constrained to integer values of the spatial frequency. Nugent proposed a refinement of this method based on library minimization routines to correct the errors in the retrieved phase when the value of the carrier frequency is noninteger.³ A requirement for this improvement to be successfully implemented is that the phase object is of only limited spatial extent, i.e., the interferogram has areas devoid of modulation, which is not true in most applications.

A variety of approaches has been proposed for carrier removal in the spatial domain. Bone et al.⁴ estimated the carrier phase by the least-squares fit (LSF) of a plane to the retrieved phase distribution in a region that has no contribution from the desired information. Then, heterodyning is removed by direct subtraction of the calculated plane in the spatial domain. If carrier fringes are undesirably twisted, a simple linear fit introduces errors. For the same case, Gu and Chen proposed a bilinear surface or some other function to describe the carrier.¹¹ Obviously, the accuracy of the retrieved phase is dramatically affected by the right choice of a particular surface. Furthermore, the requirement of an information-free region in the interferograms cannot always be fulfilled. A similar approach was suggested for the cases in which the carrier frequency can be measured or calculated (for example, by measuring the tilt angle of the mirror in the interferometer). However, generally it is not possible or is extremely difficult to obtain a reliable estimation for the carrier frequency,¹⁰ and therefore this method is not considered here. Finally, the true distribution of the carrier phase can be obtained by analyzing a fringe pattern recorded previous to the event (deformation, change of refraction index, etc.) that gives rise to the phase of interest.¹² Once the interferogram with modulated carrier fringes is recorded and analyzed, the carrier is removed by subtracting the phase of the undeformed carrier fringes (SPUCF) from the recovered phase in the spatial domain. This method is particularly well suited for the analysis of fringe patterns in which the spatial carrier frequency is a function of the spatial coordinates, i.e., unequally spaced and/or twisted carrier fringes. Nevertheless, the use of an additional fringe pattern duplicates the number of direct and inverse Fourier transforms, and hence the computing time. Also, the requirement for an additional fringe pattern makes the system sensitive to environmental disturbances, negating the advantage of the FTM over temporal phase measurement methods.

A phase algorithm without the influence of the carrier was recently demonstrated for a phase-stepping profilometry system.¹³ It makes the procedure of phase unwrapping easier because wrappings and some other discontinuities caused by the carrier frequency are removed. However, its application to other evaluation techniques, e.g., Fourier analysis of TV holography fringe patterns, is not straightforward.

3 Analysis of Computer-Generated Fringe Patterns

The use of computer-generated fringe patterns enables an exact determination of the difference between the retrieved and the desired phases, as the original phase distribution is known. For that reason, we simulated the fringe patterns following the method described in Ref. 14, which models the process of generating correlation fringe patterns for an out-of-plane TV holography (TVH) interferometer. The TVH fringe patterns were obtained for a resolution of 512×512 pixels by subtracting two speckle interferograms with a known phase difference. The average speckle size is 2 pixels.

Three different cases are considered: (1) the carrier frequency is an integer, (2) the carrier frequency is not an integer number, and (3) the carrier frequency varies continuously along the vertical direction. Two fringe patterns were generated for each case (Fig. 1), containing pure and modulated carrier fringes, respectively. The phase term that introduces modulation in the carrier fringes is a conical surface. These modulated carrier fringes represent the pattern that could be obtained from an out-of-plane TVH interferometer in which the test object undergoes an out-of-plane conical deformation and the reference beam is properly tilted. Actual values of the carrier frequencies for the generated patterns are $u = 15, 15.4$ and $14.5 + i/512$ for cases (1), (2) and (3), respectively, where i is a variable index from 1 to 512 expressing the row number. The conical phase term that represents the modulation is the same for the three cases. Its circular base (radius of 200 pixels) is placed at the center of the image and its height is $2 \times 2\pi$ rad. Hence, the external frame of the fringe pattern is free of the desired information, as required by the LSF method.

Fringe analysis and carrier removal are schematically described in Fig. 2. Fringe patterns are Fourier transformed using of a 2-D fast Fourier transform (FFT) algorithm in a PC-based image processor. Filtering is performed in the Fourier plane by multiplying the spectra by a function that yields 1 inside a circle and 0 otherwise. The frequency coordinates of the center of this circular domain are set to

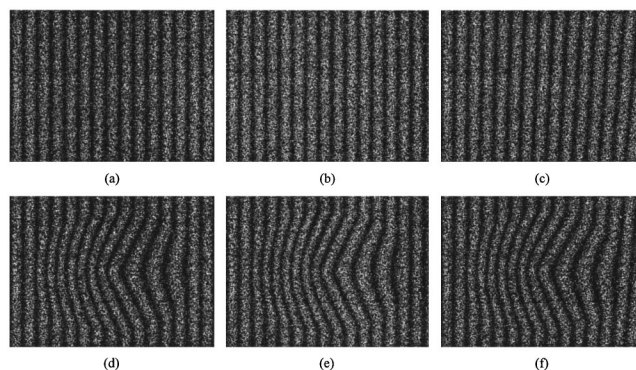


Fig. 1 Computer-generated fringe patterns: (a) to (c) undeformed carrier fringes and (d) to (f) modulated carrier fringes. The simulated deformation is a conical surface. Carrier frequencies are (a) and (d) 15, (b) and (e) 15.4 and (c) and (f) $14.5 + i/512$, where i denotes the row number.

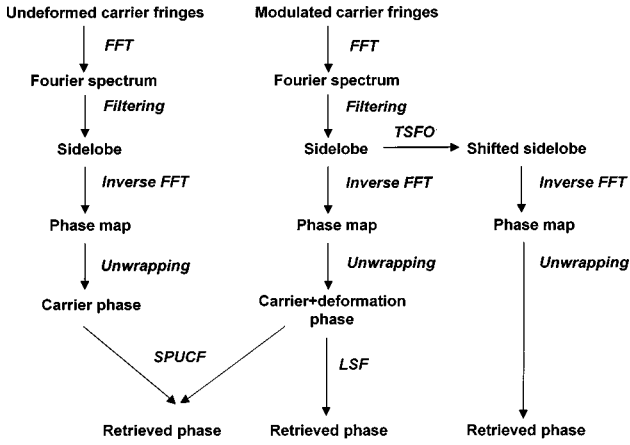


Fig. 2 Flow chart of fringe analysis by the FTM with three different methods of carrier removal: TSFO, LSF and SPUCF.

15 and 0 for the horizontal and vertical components, respectively, and the radius to 7 pixels. Moreover, $(-15,0)$ are the frequency components of the translation given to the filtered sidelobes of the three modulated fringe patterns when they are analyzed by the TSFO method. An LSF over an area of the fringe pattern formed by lines 1 to 50, lines 463 to 512, columns 1 to 50 and columns 463 to 512 is used to calculate the plane that represents the carrier phase in the LSF method for the fringe patterns in Figs. 1(d) to 1(f).

4 Assessment of Methods

We took into account only phase errors due to carrier removal because the aim of our paper is to quantitatively compare the accuracy of three carrier removal methods: TSFO, LSF and SPUCF. The influence of error sources other than carrier removal, for example, carrier frequency determination or spatial frequency bandwidth, is the same for the three methods and it is not considered here.

To assess the performance of the TSFO, LSF and SPUCF methods, several figures of merit were used. Their descriptions and expressions are listed in Table 1, where $\varphi(i,j)$ represents the original phase and $\varphi'(i,j)$ the retrieved phase for a pixel placed at the i 'th row and the j 'th

column of the image. Relevant information can be obtained from the modulus of the difference between the retrieved and original phase distributions. The mean and maximum values as well as the standard deviation of the absolute error are calculated. The parameter called fidelity quantifies how well details are preserved.¹⁵ Additional insight can be gained by means of the relative mean absolute error, which measures the relative weight of the errors. Values close to 1 are desirable for fidelity and close to 0 for the rest of parameters. Actual values of the parameters just mentioned are shown in Table 2. The TSFO, LSF and SPUCF methods were tested over three different couples of computed-simulated fringe patterns, as explained in the previous section, resulting in nine values for each parameter. In addition to the numerical values, plots of the phase errors along the central row of the phase maps are shown in Fig. 3. In agreement with the arguments given in Section 2, the phase yielded by TSFO contains linear errors when the carrier frequency is noninteger [Fig. 3(c)]. Linear errors also occur when the phase is calculated by LSF whichever the carrier frequency is [Figs. 3(b) to 3(d)]. In this case, these errors are caused by using pixels from the edge of the fringe pattern domain to calculate the plane coefficients.

5 Application Example

Transient deformations can be qualitatively studied¹⁶ with standard pulsed TVH. In a recent paper, we reported an improvement of a standard pulsed TVH system that enables quantitative measurements of transient bending waves to be performed.¹⁷ The spatial carrier is introduced in the fringe patterns using a novel optical setup that separates and recombines the object beams from a twin-cavity diode-seeded Nd:YAG pulsed laser. A detailed description of the experimental setup, spatial carrier generation and fringe analysis is provided in Ref. 17.

The aim of this section is to quantify the differences that arise due to carrier removal in real measurements of transient bending waves. Fig. 4(a) shows a correlation fringe pattern obtained¹⁷ by double-pulsed-subtraction TVH for a metal plate impact-excited with a piezoelectric translator. Vertical carrier fringes are modulated by the deformation undergone by the plate $\approx 20 \mu\text{s}$ after mechanical excitation. The spatial carrier frequency is calculated from Fourier spectrum of the fringe pattern. The fringes are ana-

Table 1 Figures of merit for a known phase distribution.

Description	Expression
Mean absolute error	$ e _{\text{ave}} = \frac{\sum_{i=1}^{512} \sum_{j=1}^{512} \varphi(i,j) - \varphi'(i,j) }{512 \times 512}$
Standard deviation of the absolute error	$\sigma_{ e } = \left\{ \frac{\sum_{i=1}^{512} \sum_{j=1}^{512} [\varphi(i,j) - \varphi'(i,j) - e _{\text{ave}}]^2}{512 \times 512 - 1} \right\}^{1/2}$
Maximum absolute error	$ e _{\text{max}} = \max[\varphi(i,j) - \varphi'(i,j)], 1 \leq i, j \leq 512$
Fidelity	$f = 1 - \frac{\sum_{i=1}^{512} \sum_{j=1}^{512} \varphi(i,j) - \varphi'(i,j) ^2}{\sum_{i=1}^{512} \sum_{j=1}^{512} \varphi(i,j)^2}$
Relative mean absolute error	$r = \frac{1}{512 \times 512} \frac{\sum_{i=1}^{512} \sum_{j=1}^{512} \varphi(i,j) - \varphi'(i,j) }{\sum_{i=1}^{512} \sum_{j=1}^{512} \varphi(i,j)}$

Table 2 Numerical comparison of TSFO, LSF and SPUCF carrier removal methods for computer-generated fringe patterns with three different carrier frequencies.

Carrier Frequency	$u=15$			$u=15.4$			$u=14.5+i/512$		
	TSFO	LSF	SPUCF	TSFO	LSF	SPUCF	TSFO	LSF	SPUCF
$ e _{ave}(\times 2\pi \text{ rad})$	0.02307	0.13849	0.01551	0.20798	0.13921	0.01716	0.13321	0.22277	0.01553
$\sigma e (\times 2\pi \text{ rad})$	0.01690	0.09349	0.01546	0.11548	0.09666	0.01687	0.11061	0.14132	0.01594
$ e _{max}(\times 2\pi \text{ rad})$	0.10630	0.41562	0.37402	0.46457	0.42430	0.34252	0.56693	0.73885	0.38189
f	0.99742	0.91203	0.99849	0.82170	0.90949	0.99818	0.90565	0.78074	0.99844
$r(\times 10^{-6})$	0.2762	1.6579	0.1857	2.4898	1.6664	0.2054	1.5947	2.6668	0.1860

lyzed by the FTM, resulting in a deformation plus carrier phase map [Fig. 4(b)]. The LSF method performs a least-squares plane fit over an external frame devoid of modulation (described in Section 3). A 3-D plot of transient deformation after phase unwrapping and carrier removal by

SPUCF is presented in Fig. 4(c). In contrast to computer-generated fringe patterns, the exact value of transient deformation is unknown, so it is not possible to measure absolute errors due to carrier removal in the analysis of experimental fringes. Instead, differences between phase

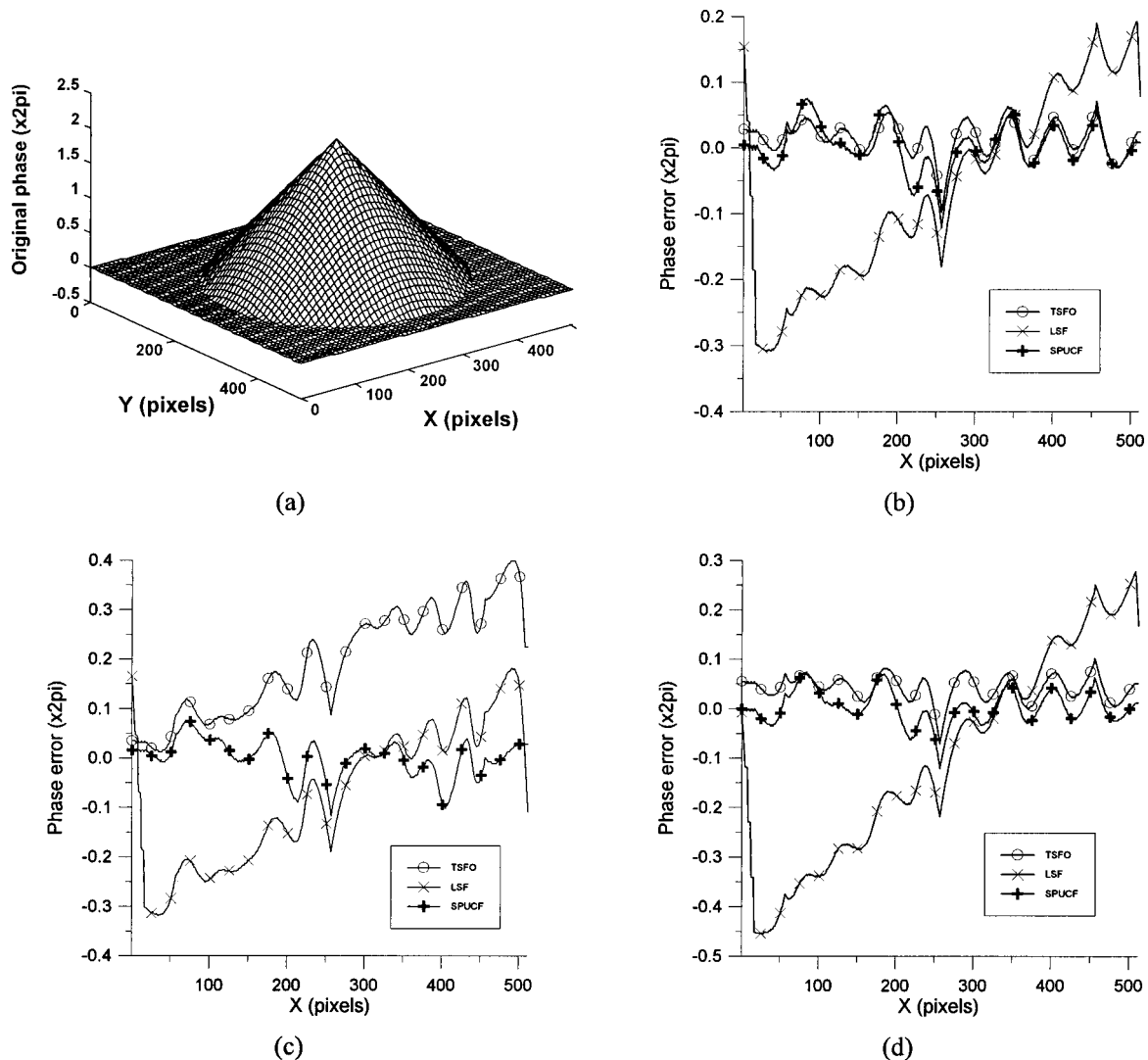


Fig. 3 (a) Three-dimensional plot of the computer-generated phase distribution and (b) to (d) plots of the phase errors along the central row for the carrier frequencies: (b) 15, (c) 15.4 and (d) 14.5 + $i/512$.

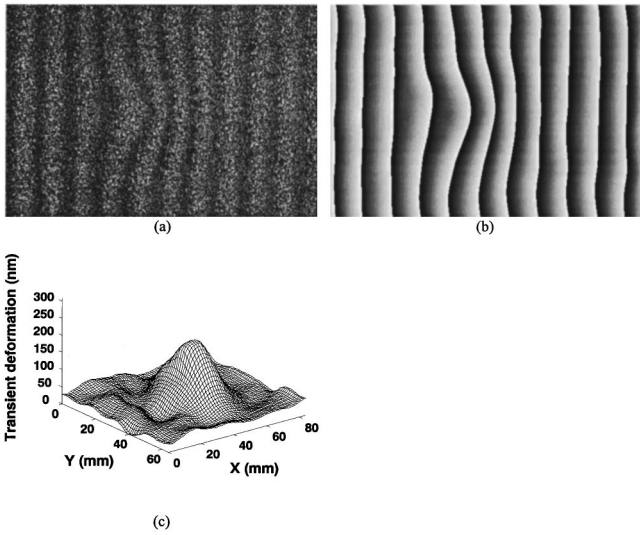


Fig. 4 Experimental results: (a) correlation fringe pattern obtained by double-pulsed-subtraction TVH $\approx 20 \mu\text{s}$ after a metal plate receives the impact of a piezoelectric translator; (b) phase map, deformation plus carrier; and (c) 3-D plot of transient deformation after phase unwrapping and carrier removal by SPUCF.

distributions obtained by two different carrier removal methods are calculated. The phase differences plotted at Figs. 5(a) and 5(b) stress two facts. First, the use of different carrier removal methods in the analysis of experimental fringe patterns by the FTM gives rise to significant differences in the recovered phase, and second, these differences are more relevant along the direction of the spatial carrier. Figures of merit listed in Table 1 are inappropriate to assess the accuracy of the TSFO, LSF and SPUCF methods when applied to experimental fringes because absolute errors are unknown. A further approach to evaluate the performance of these methods over real fringes is to calculate the deviation of the measurements, defined as:

$$d(i,j) = \varphi'_{\max}(i,j) - \varphi'_{\min}(i,j), \quad (1a)$$

$$\varphi'_{\max}(i,j) = \max[\varphi'_{\text{TSFO}}(i,j), \varphi'_{\text{LSF}}(i,j), \varphi'_{\text{SPUCF}}(i,j)] \quad (1b)$$

$$\varphi'_{\min}(i,j) = \min[\varphi'_{\text{TSFO}}(i,j), \varphi'_{\text{LSF}}(i,j), \varphi'_{\text{SPUCF}}(i,j)], \quad (1c)$$

where $\varphi'_{\text{TSFO}}(i,j)$, $\varphi'_{\text{LSF}}(i,j)$ and $\varphi'_{\text{SPUCF}}(i,j)$ are the phases retrieved by the TSFO, LSF and SPUCF carrier removal methods, respectively. The term $d(i,j)$ has the physical meaning of an upper limit for the difference between two measurements, whichever method is used for carrier removal. The actual values of the maximum, minimum, mean and standard deviation of $d(i,j)$ are listed in Table 3, expressed in both radians and nanometers.

6 Discussion and Conclusions

Numerical data in Table 2 reveal that SPUCF is the carrier removal method that introduces less error in the phase distribution for the computer-generated fringes analyzed in this paper. In the studied example, the fidelity of the retrieved phase is always greater than 99% when SPUCF is used. Furthermore, it yields the lowest values of $|e|_{\text{ave}}$, $\sigma_{|e|}$ and r for the three cases compared. SPUCF can be used in the analysis of interferograms both with and without an area devoid of phase information. We can conclude that SPUCF is the most accurate carrier removal method in Fourier fringe analysis, and must be used if possible, i.e., if the environmental disturbances between the recording of undeformed and modulated carrier fringes are neglectable.

Note that particular cases exist in which the preceding conclusions are not valid. For example, if the carrier frequency must be calculated from an extended spectrum, TSFO is not accurate. Phase distributions with a linear term are another exception, because in this case, TSFO and SPUCF do not perform correctly.

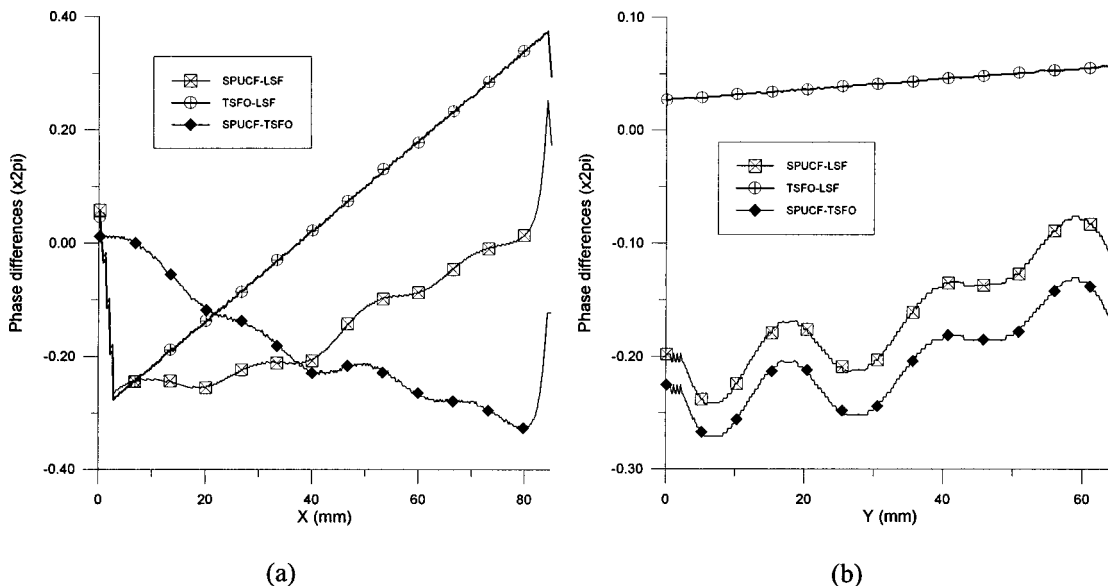


Fig. 5 Experimental results for the differences between retrieved phases obtained by two different carrier removal methods: cross section along (a) the central row and (b) the central column.

Table 3 Figures of merit for an unknown phase distribution.

Parameter	Actual Value ($\times 2\pi$ rad)	Actual Value (nm)
$d_{\max} = \max[d(i,j)], 1 \leq i, j \leq 512$	0.4020	106.93
$d_{\min} = \min[d(i,j)], 1 \leq i, j \leq 512$	0.0310	8.25
$d_{\text{ave}} = \frac{\sum_{i=1}^{512} \sum_{j=1}^{512} d(i,j)}{512 \times 512}, 1 \leq i, j \leq 512$	0.2471	65.72
$\sigma_d = \left\{ \frac{\sum_{i=1}^{512} \sum_{j=1}^{512} [d(i,j) - d_{\text{ave}}]^2}{512 \times 512 - 1} \right\}^{1/2}, 1 \leq i, j \leq 512$	0.0665	17.68

The choice between TSFO and LSF in applications where SPUCF is unsuitable must be made with regard to the particular spatial carrier. If the value of the carrier frequency is integer, TSFO exhibits better performance than LSF. However, this assumption is not true in practice. For the general case of a noninteger carrier frequency, TSFO introduces greater errors in the retrieved phase than LSF. This is due to the ‘‘picket fence’’ effect.⁶ Nevertheless, if the carrier frequency varies continuously across the fringe pattern, TSFO is more accurate than LSF. This is so because the spectrum of a continuously varying carrier frequency is spread across the Fourier plane rather than being concentrated in a discrete point, and then some of the spectrum energy is located on the sampled frequencies or near them. TSFO is also more advantageous than LSF in that the unwrapping procedure is easier, especially for the case of high carrier frequencies, because wrappings and poles due to the spatial carrier are removed from the phase maps.¹³

The results of this study can be summarized as follows. Errors due to carrier removal must be taken into account when using the FTM for phase evaluation in high precision measurement systems. SPUCF is the most accurate carrier removal method in Fourier fringe analysis. If immunity to external disturbances is critical in the application, either TSFO or LSF must be used. The right choice of method is determined by the particular carrier frequency that is encoded in the fringe patterns. LSF is advisable only when the frequency of the carrier fringes is constant and noninteger.

Acknowledgments

The authors thank the following institutions for their support: Xunta de Galicia (XUGA 32101B95), Comisión Interministerial de Ciencia y Tecnología (TAP95-0805-E) and Universidade de Vigo. Part of this work was presented at the Applied Optics Divisional Conference of the Institute of Physics.¹⁸

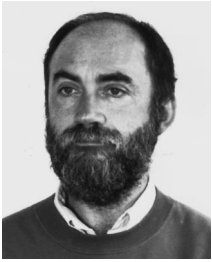
References

1. M. Takeda, H. Ina, and S. Kobayashi, ‘‘Fourier-transform method of fringe-pattern analysis for computer-based topography and interferometry,’’ *J. Opt. Soc. Am.* **72**, 156–160 (1982).
2. M. Kujawinska, ‘‘Spatial phase measurement methods,’’ in *Interferogram Analysis*, D. W. Robinson and G. T. Reid, Eds., pp. 141–193, IOP Publishing Ltd., Bristol (1993).
3. K. A. Nugent, ‘‘Interferogram analysis using an accurate fully automatic algorithm,’’ *Appl. Opt.* **24**, 3101–3105 (1985).
4. D. J. Bone, H.-A. Bachor, and J. Sandeman, ‘‘Fringe-pattern analysis

- using a 2-D Fourier transform,’’ *Appl. Opt.* **25**, 1653–1660 (1986).
5. R. J. Green, J. G. Walker, and D. W. Robinson, ‘‘Investigation of the Fourier-transform method of fringe pattern analysis,’’ *Opt. Lasers Eng.* **8**, 29–44 (1988).
6. D. R. Burton and M. J. Lalor, ‘‘Managing some of the problems of Fourier fringe analysis,’’ *Proc. SPIE* **1163**, 149–160 (1989).
7. M. Kujawinska and J. Wójciak, ‘‘High accuracy Fourier transform fringe pattern analysis,’’ *Opt. Lasers Eng.* **14**, 325–339 (1991).
8. X. Li, Z. Zhang, and X. Wu, ‘‘Investigation of the Fourier transform method in analysis of photo-carrier fringe patterns,’’ *Proc. SPIE* **2544**, 343–353 (1995).
9. G. Lai and T. Yatagai, ‘‘Use of the fast Fourier transform method for analyzing linear and equispaced Fizeau fringes,’’ *Appl. Opt.* **33**, 5935–5940 (1994).
10. R. W. T. Preator and R. Swain, ‘‘Fourier transform fringe analysis of electronic speckle pattern interferometry fringes from high-speed rotating components,’’ *Opt. Eng.* **33**, 1271–1279 (1994).
11. J. Gu and F. Chen, ‘‘Fast Fourier transform, iteration, and least-squares-fit demodulation image processing for analysis of single-carrier fringe pattern,’’ *J. Opt. Soc. Am. A* **12**, 2159–2164 (1995).
12. J. M. Huntley and J. E. Field, ‘‘High resolution moire photography: application to dynamic stress analysis,’’ *Opt. Eng.* **28**, 926–933 (1989).
13. H.-J. Su, J. L. Li, and X.-Y. Su, ‘‘Phase algorithm without the influence of carrier frequency,’’ *Opt. Eng.* **36**, 1799–1805 (1997).
14. A. Dávila, G. H. Kaufmann, and D. Kerr, ‘‘Digital processing of ESPI addition fringes,’’ in *Proc. 2nd. Int. Workshop on Automatic Processing of Fringe Patterns*, W. Jüptner and W. Osten, Eds., pp. 339–346, Akademie Verlag, Berlin (1993).
15. A. Dávila, G. H. Kaufmann, and D. Kerr, ‘‘Scale-space filter for smoothing electronic speckle pattern interferometry fringes,’’ *Opt. Eng.* **35**, 3549–3554 (1996).
16. A. Fernández, A. J. Moore, C. Pérez-López, A. F. Doval, and J. Blanco-García, ‘‘Study of transient deformations with pulsed TV holography: application to crack detection,’’ *Appl. Opt.* **36**, 2058–2065 (1997).
17. A. Fernández, J. Blanco-García, A. F. Doval, J. Bugarín, B. V. Dorrió, C. López, J. M. Alén, M. Pérez-Amor, and J. L. Fernández, ‘‘Transient deformation measurement by double-pulsed-subtraction TV holography and the Fourier transform method,’’ *Appl. Opt.* **37**, 3440–3446 (1998).
18. A. Fernández, G. H. Kaufmann, and A. F. Doval, ‘‘Comparison of carrier removal methods in Fourier transform fringe analysis,’’ in *Proc. Appl. Opt. Div. Conf. of The Institute of Physics*, K. T. V. Grattan, Ed., pp. 11–16, Institute of Physics Publishing (1998).



Antonio Fernández received his Industrial Engineer degree in 1993 and his Doctor of Industrial Engineering degree in 1998, both from the Universidade de Vigo, Spain. His main research interests are TV holography and related techniques, fringe pattern analysis and digital image processing. He is a member of SPIE.



Guillermo H. Kaufmann received his DSc degree in physics in 1978 from the Universidad de Buenos Aires, Argentina. He is currently a professor with the Physics Department of the Universidad Nacional de Rosario and a research scientist with the Consejo Nacional de Investigaciones Científicas y Técnicas, Argentina. He also heads the Division of Experimental and Applied Physics of the Instituto de Física Rosario, where he leads a group

working in optical metrology. He has been a visiting researcher with the National Physical Laboratory, United Kingdom, the University of Michigan, the Swiss Federal Institute of Technology at Lausanne, the University of Cambridge, the Mechanical Engineering Laboratory in Japan and Loughborough University, United Kingdom. Prof. Kaufmann has authored three book chapters and more than 70 scientific papers published in refereed journals and conference proceedings. His major research interests include the development of coherent optics techniques for strain analysis and nondestructive testing, speckle metrology, phase shifting interferometry, fringe analysis and digital image processing. He is a member of OSA, SPIE and IEEE.



Ángel F. Doval is a lecturer in applied physics with the Universidade de Vigo, Spain. He received his Industrial Engineer degree from the University of Santiago de Compostela in 1990 and his Doctor in Industrial Engineering degree from the Universidade de Vigo in 1997. His main research interests are TV holography (electronic speckle pattern interferometry) and related techniques, fringe pattern analysis, and the use of fiber optics and laser diodes in interferometric systems.



Jesús Blanco-García received his doctoral degree in physics in 1992 with a thesis on holographic interferometry from the University of Santiago de Compostela. He currently teaches general physics at the Universidade de Vigo. His main research subjects are TV holography, holographic interferometry, moiré methods, interferometers and fringe analysis.



José L. Fernández received his diploma in mechanical engineering from the Universidad Politécnica de Madrid in 1984 and has since been with the Optical Metrology Group of the Industrial Engineering School of Vigo, which until 1989 was affiliated with the Universidad de Santiago de Compostela, where he received his PhD degree in engineering in 1988. He is currently a senior lecturer with the Industrial

Engineering School of Vigo, now part of the Universidade de Vigo. His interests include dimensional measurements and nondestructive inspection by optical means and, more specifically, cw and pulsed TV holography, interferometry and moiré techniques.